

~~CONFIDENTIAL~~

RM A54F22

NACA RM A54F22



# RESEARCH MEMORANDUM

AN EXPERIMENTAL INVESTIGATION OF REDUCTION IN TRANSONIC  
DRAG RISE AT ZERO LIFT BY THE ADDITION OF VOLUME TO  
THE FUSELAGE OF A WING-BODY-TAIL CONFIGURATION  
AND A COMPARISON WITH THEORY

By George H. Holdaway

Ames Aeronautical Laboratory  
Moffett Field, Calif.

CLASSIFICATION CHANGED

**LIBRARY COPY**

To UNCLASSIFIED

AUG 19 1954

LANGLEY AERONAUTICAL LABORATORY  
LIBRARY, ROOM  
LANGLEY FIELD, VIRGINIA

By authority of NACA Res 24  
4 RN-121

Date: Dec 14, 1957

CLASSIFIED DOCUMENT

This material contains information affecting the National Defense of the United States within the meaning of the espionage laws, Title 18, U.S.C., Secs. 793 and 794, the transmission or revelation of which in any manner to an unauthorized person is prohibited by law.

## NATIONAL ADVISORY COMMITTEE FOR AERONAUTICS

WASHINGTON

August 18, 1954

~~CONFIDENTIAL~~

## NATIONAL ADVISORY COMMITTEE FOR AERONAUTICS

RESEARCH MEMORANDUMAN EXPERIMENTAL INVESTIGATION OF REDUCTION IN TRANSONIC  
DRAG RISE AT ZERO LIFT BY THE ADDITION OF VOLUME TO  
THE FUSELAGE OF A WING-BODY-TAIL CONFIGURATION  
AND A COMPARISON WITH THEORY

By George H. Holdaway

## SUMMARY

An experimental investigation was made by the free-fall recoverable-model technique to assess at zero lift the possibilities of reducing the drag-rise coefficients of a wing-body-cruciform-tail combination by adding volume to the fuselage. The basic features of the test model were an unswept aspect-ratio-3.1 thin wing, a fineness-ratio-12.4 fuselage, and four  $45^\circ$  sweptback tail surfaces. The tests covered a Mach number range of 0.84 to 1.15 with Reynolds numbers of 6,000,000 to 14,000,000, based on the wing mean aerodynamic chord.

Considerable reduction in drag-rise coefficient was effected for several different modifications by the addition of properly distributed volume to the fuselage. In one instance, a reduction in drag coefficient was obtained by adding a volume which was almost four times the exposed wing volume. The computation method presented in NACA RM A53H17 generally predicted the supersonic drag-rise coefficients for each modification within 20 percent of the experimental values. As in the above-mentioned report, the predictions at a Mach number of one were not accurate. The changes in drag-rise coefficients resulting from the modifications were generally predicted with better accuracy than the values of drag-rise coefficients.

## INTRODUCTION

During the past year, fuselage indentations of the "area-rule" type have successfully reduced the transonic zero-lift drag-rise coefficients of numerous wing-fuselage combinations. A summary of the earlier results is presented in reference 1. In some cases, where minimum diameters are controlled by the engine or other components, fuselage indentation is not feasible. Also, for existing aircraft, indentation may be impractical, if not impossible. These facts led to the concept of increasing the

fuselage volume in proper regions to produce drag reductions comparable to those obtained by indentation. An indication that this concept would be feasible was obtained independently by an experiment reported in reference 1 and by an analysis presented in reference 2. The results of reference 1 included a case where the drag-rise coefficient of an airplane model was significantly reduced by lengthening the fuselage and by adding volume to improve the area distribution of the rearward portion of the model; a further reduction was obtained by filling a dip in the area distribution for the forward portion of the model.

The procedure followed in the analytical approach was to use the calculation method of reference 2, which is based on the theory of reference 3, to determine if reductions of drag-rise coefficients are possible with addition of volume to the fuselage, and to determine what modifications would indicate sufficient gains to warrant experimental investigation. The configuration studied was an aspect-ratio-3.1 unswept wing on a fineness-ratio-12.4 fuselage with a cruciform tail. The more promising modifications to the fuselage were those designed for minimum drag for the configuration at Mach numbers 1.00, 1.05, and 1.14. This analysis, presented in reference 2, indicated that addition of volume to the fuselage would result in substantial reduction in drag-rise coefficients, even at supersonic speeds for the  $M=1.05$  and  $M=1.14$  modifications.

The investigation of this report was undertaken to provide experimental data for comparison with the predictions presented in reference 2. The experimental results would provide additional data for a quantitative assessment of the computation method, and would indicate the degree to which the reductions in wave-drag coefficients indicated by theory could be achieved as measured reductions in drag-rise coefficients.

The tests were made by the Ames Aeronautical Laboratory at the facilities of the Edwards Air Force Base using the free-fall recoverable-model technique. The models tested were of large scale resulting in Reynolds numbers of 6,000,000 to 14,000,000, based on the wing mean aerodynamic chord, for the test Mach number range of  $M=0.84$  to  $M=1.15$ .

#### SYMBOLS

- $C_{D_0}$  zero-lift drag coefficient,  $\frac{\text{drag at zero lift}}{qS_w}$
- $C_{D_0}'$  zero-lift wave-drag coefficient,  $\frac{\text{theoretical wave drag at zero lift}}{qS_w}$
- $\Delta C_{D_0}$  zero-lift drag-rise coefficient,  $\frac{\Delta D_0}{qS_w}$
- $c$  local chord measured parallel to plane of symmetry

$\bar{c}_w$	mean aerodynamic chord of the total wing
$\Delta D_0$	zero-lift drag rise above subsonic drag level
$H$	total pressure in the boundary layer
$H_0$	free-stream total pressure
$M$	free-stream Mach number
$q$	free-stream dynamic pressure
$R$	Reynolds number based on $\bar{c}_w$
$S$	projection of $S_s$ on a plane perpendicular to $x$ axis
$S_s$	cross-sectional areas formed by cutting the configurations with planes perpendicular or oblique to the $x$ axis
$S_w$	total wing area
$U$	velocity at the edge of boundary layer
$u$	velocity in the boundary layer
$x$	Cartesian coordinate as conventional body axis
$y$	distance measured normal to the fuselage surface
$\delta$	boundary-layer displacement thickness

#### MODELS

The dimensions of the unmodified model are given in figure 1, and the radii of the fineness-ratio-12.4 fuselage are listed in table I. Additional details of the  $45^\circ$  sweptback tail surfaces are given in reference 2. The wing used in the investigation was unswept with an aspect ratio of 3.1, a taper ratio of 0.39, and a total plan-form area of 21.68 square feet. The wing section was elliptical from 0 to 0.5 of the local chord and biconvex from 0.5 chord to the trailing edge. The maximum wing thickness-to-chord ratio was 3 percent. The wing had no twist, dihedral, or incidence, and was of solid aluminum alloy construction. The fuselage radii defined in figure 1 are for a minimum-drag body of revolution for given volume and length (Sears-Haack body), but behind fuselage station 139.4 the theoretical radii and fuselage length were extended as dictated by the space required for the recovery mechanism.

The fuselage radii for the three modifications designed to provide minimum wave-drag coefficients for Mach numbers 1.00, 1.05, and 1.14 are presented in table I. The axial distributions of cross-sectional area normal to the longitudinal axis for the basic model and for the three modifications are presented in figure 2. The model modified for  $M=1.00$  is shown in figure 3 to illustrate the comparative size of the model and the fact that the changes in radii are quite gradual even though the volume added is large. All cross sections were maintained circular as in the original configuration. Although the general design procedure was presented in reference 2, more detailed comments are included in this report describing the specific modifications.

#### Modification 1, for $M=1.00$

Volume was added to the fuselage to alter the normal cross-sectional area distribution of the original configuration to that for a Sears-Haack body with the same maximum cross-sectional area (fig. 4(a)). In this case, the values of projected cross-sectional area  $S$  are, of course, identical with the values of cross-sectional area  $S_p$  formed by perpendicular cutting planes.

The type of body shape used for the modification was the same as that for the original fuselage (Sears-Haack body; i.e., minimum-drag body of revolution for given length and volume), so that the investigation would not be affected by an additional variable. The equation for the body radii (fig. 1) differed only in that the maximum radius was increased. An additional advantage of the body shape used was that the ends of this type of Sears-Haack body are less slender than some other minimum drag shapes and would more effectively fair in the bulges in the area-distribution curve due to the tail. Modifications were not made behind fuselage station 165 because fuselage indentation would be involved and this was not practical because this section contained the recovery mechanism.

The volume added to the fuselage was 3.63 cubic feet or almost four times the exposed wing volume of 0.92 cubic feet.

#### Modifications 2 and 3, for $M=1.05$ and $M=1.14$

The design procedure was similar to that used for modification 1, in that volume was added to an area-distribution curve to provide a similar Sears-Haack shape; however, the procedure differed with respect to the type of area-distribution curves used to determine the modification.

The area-distribution curves used were average curves based on average projected values of  $S_p$  obtained with cutting planes tangent to the design

Mach cones. The theory upon which this method is based is discussed in reference 3. The resultant average area-distribution curves for the design Mach numbers are shown in parts (b) and (c) of figure 4, with the volume added for each modification.

The volume added to the fuselage was approximately three times the exposed wing volume for the  $M=1.05$  modification, and twice that volume for the  $1.14$  modification.

It should be noted that the average area-distribution curves were used only in determining the modifications and were not used in computing the drag. The individual curves prior to averaging were used to predict the wave-drag coefficients.

#### INSTRUMENTATION

Drag measurements were made with two sensitive NACA recording accelerometers which are accurate to  $\pm 0.0025$  g, producing an expected instrument accuracy of  $C_D = \pm 0.0004$  at  $M=1.00$  and  $C_D = \pm 0.0002$  at  $M=1.14$ . Accelerometer 1 was located slightly above, and accelerometer 2 slightly below, the model center of gravity.

Pressure measurements were made with a six-cell recording manometer which was accurate within  $\pm 0.05$  inch of mercury for pressure readings near zero, and was accurate within 2 percent of the full-scale value of 15 inches of mercury. Mach number was obtained from a calibrated airspeed head and was considered to be accurate within  $M \pm 0.01$ . A four-tube pitot-pressure rake (fig. 5) was located at fuselage station 100 to measure the boundary-layer profile. Tube openings were located about 0.1, 0.3, 0.6, and 0.9 inch from the fuselage surface. For two of the tests, base pressures were determined by manifolding orifices located using an area-weighted basis as shown in figure 6.

All records taken within the model were synchronized by means of a 1/10-second chronometric timer.

#### TESTS

The models were released from a carrier airplane at an altitude of 40,000 feet and allowed to fall freely without propulsion. All surfaces were trimmed for zero lift and recovery was initiated at a safe altitude. The first two flights were tests of modifications 1 and 2 which were designed for  $M=1.00$  and  $M=1.05$ , respectively. The third flight was a test of the modification for  $M=1.05$  with the tail fairing behind fuselage

station 190-5/8 cut off to form a flat base. This latter test was made to provide data for correlation with possible wind-tunnel tests, and the base pressure was measured with four pressure orifices manifolded together and located near the center of the base as shown in figure 6(a).

The last flight was a test of modification 3 for  $M=1.14$ . For this flight, an effort was made to obtain an indication of the pressure drag of the tail fairing which also would be of interest in obtaining approximate forebody drag for comparison with possible wind-tunnel tests. Seven orifices were located as shown in figure 6(b) to represent equal portions of projected area for a base diameter of 10-1/8 inches. These orifices were manifolded together by a large diameter tube (7/8-inch inside diameter).

The Reynolds number variation with Mach number for the series of tests is given in figure 7.

### RESULTS

The experimental results for the three test configurations with tail fairing are presented in figure 8. Included in this figure are the theoretical curves of wave-drag coefficients obtained from reference 2. The experimental values of subsonic drag coefficients were used to establish the datum above which the theoretical wave-drag coefficients were plotted. Comparing the experimental and theoretical drag coefficients in this manner is equivalent to assuming that the level of friction-drag coefficient is constant for each modification over the test range of Mach numbers and Reynolds numbers. This assumption was considered to be justified because a cursory check by available theories indicated that the variation of friction-drag coefficient would be of the same order of magnitude as the accuracy of the experimental total-drag coefficients. The assumption was further justified for the purpose of comparing modifications, since the variation of friction-drag coefficient would be similar for each modification. The tail-fairing drag, presented in figure 8(c), was calculated using the manifold pressure from the seven pressure orifices which were located on an area weighted basis. The experimental results for the modification for  $M=1.05$  with the blunt tail are presented in figure 9. Paired curves of the experimental data for the three modifications are presented in figure 10. Also included in this figure are the experimental data from reference 2 for the unmodified configuration.

The theoretical results for the three modifications and the original model, obtained from reference 2, are repeated in figure 11 for convenience in making comparisons.

Total-pressure distributions in the boundary layer at fuselage station 100 are presented in figure 12, for the three modifications. The boundary-layer displacement thickness,  $\delta$ , for each modification was estimated from this figure.

## DISCUSSION

A comparison was made between the experimental drag-rise coefficients and predicted wave-drag coefficients computed by the method of reference 2. The results of this comparison at four Mach numbers are tabulated in table II and plotted in figure 13. The supersonic drag-rise coefficients from  $M=1.02$  to  $1.14$  were generally predicted within 20 percent of the experimental values. The experimental drag-rise coefficients at these supersonic speeds were generally higher than predicted, but this relationship might vary for configurations other than those tested. At supersonic speeds the maximum deviation of theory from experiment was 23.7 percent for the unmodified configuration (table II). The test data for this latter case were taken from reference 2 and are not quite as accurate as the test data for the three modifications. At a Mach number of one the experimental values were always less than the computed values and were poorly predicted for all but the  $M=1.00$  modification.

Of prime interest in this investigation was an evaluation of the effectiveness of the modifications to reduce the drag-rise coefficients by adding volume. As shown in figure 10, all the modifications resulted in reductions in drag coefficient over the Mach number range of the tests despite the fact that they represent additions of volume from two to four times the volume of the exposed wing. This result was in accordance with the computed results for all cases except for the  $M=1.00$  modification. For the  $M=1.00$  modification, a crossover of the drag-coefficient curve with that for the unmodified case was expected at  $M=1.05$  (see fig. 11), but the experimental data indicated that the crossover would not occur until a Mach number of about  $1.13$ , slightly beyond the test range. This was traceable to the fact that the drag-coefficient rise for the unmodified configuration was larger than predicted and the drag-coefficient rise for the  $M=1.00$  modification, above  $M=1.10$ , was less than predicted.

The relative order of drag-coefficient rise for each modification was in accordance with the computed results except for the fact that at a Mach number of one the  $M=1.05$  modification, even with the cut-off fuselage, had a lower drag coefficient than the  $M=1.00$  modification (which should have the minimum drag coefficient at this Mach number, as indicated by the computed results presented in figure 11). This result is attributed to the tendency, previously noted in connection with figure 13, for the computed values to be least accurate at  $M=1.00$ . It would be of interest to study this phenomenon by tests of other wing configurations with a fuselage modification for  $M=1.05$ .

The quantitative comparison between the computed and experimental improvement in drag-rise coefficients effected by the several modifications to the original configuration is presented in table III and summarized in figure 14. The differences between modifications 2 and 3 are included to



illustrate the possibility of experimentally realizing, to a degree, small changes in computed benefits. The results show that the computations tended to underestimate the benefits due to the modifications by values of drag coefficient from 0.001 to 0.002, with few exceptions. Even at a Mach number of one, the accuracies (in increments of drag coefficient) with which the differences between configurations were estimated tended to be better than the accuracies with which the drag coefficients of the individual configurations were estimated.

Prior to making the tests, it was anticipated that a separation of the boundary layer might be caused by the local pressure gradients on the body introduced by body shaping; this would introduce drag changes not accounted for by the theory. The boundary-layer measurements showed no indication of separation even for the  $M=1.00$  modification (which was the most severe change) as indicated by the typical boundary-layer velocity ratios presented in figure 15. All the profiles obtained indicated that the boundary layer was turbulent at fuselage station 100 where the measurements were obtained. This is apparent from the agreement between the data points and the theoretical curve for turbulent flow.

#### SUMMARY OF RESULTS

This investigation, utilizing tests of free-fall models at transonic speeds to assess at zero lift the possibilities of reducing the drag-rise coefficients of an unswept wing-body-tail combination by adding volume to the fuselage, has produced the following results:

1. Considerable reduction in drag-rise coefficient was effected by the addition of properly distributed volume to the fuselage. In one instance, a reduction in drag coefficient was obtained by adding a volume which was almost four times the exposed wing volume.
2. The computation method presented in NACA RM A53H17 generally predicted the supersonic drag-rise coefficients for each modification within 20 percent of the experimental values. As in the above-mentioned report, the predictions at a Mach number of one were not accurate.
3. The changes in drag-rise coefficient resulting from the modifications were generally predicted with better accuracy than the values of drag-rise coefficients.

Ames Aeronautical Laboratory  
National Advisory Committee for Aeronautics  
Moffett Field, Calif., June 22, 1954

## REFERENCES

1. Whitcomb, Richard T.: Recent Results Pertaining to the Application of the "Area Rule." NACA RM L53I15a, 1953.
2. Holdaway, George H.: Comparison of Theoretical and Experimental Zero-Lift Drag-Rise Characteristics of Wing-Body-Tail Combinations Near the Speed of Sound. NACA RM A53H17, 1953.
3. Jones, Robert T.: Theory of Wing-Body Drag at Supersonic Speeds. NACA RM A53H18a, 1953.

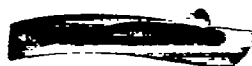


TABLE I.- FUSELAGE ORDINATES OF TEST MODELS

Fuselage station	Fuselage radii			
	Unmodified	Modification 1 for M=1.00	Modification 2 for M=1.05	Modification 3 for M=1.14
0	1.19	1.19	1.19	1.19
2	1.36	1.36	1.36	1.36
4	1.57	1.57	1.57	1.57
5	1.70	1.70	1.70	1.70
7.5	2.04	2.25	2.18	2.12
10	2.41	2.78	2.70	2.64
20	3.89	4.48	4.36	4.26
30	5.07	5.82	5.67	5.55
40	6.01	6.91	6.74	6.59
50	6.78	7.80	7.60	7.43
60	7.40	8.49	8.28	8.10
70	7.86	9.04	8.81	8.58
80	8.20	9.42	9.05	8.65
85	8.32	9.33	8.83	8.56
90	8.41	8.99	8.62	8.48
95	8.47	8.61	8.53	8.47
102	8.50	8.50	8.50	8.50
105	8.49	8.58	8.51	8.51
110	8.46	8.95	8.65	8.57
115	8.40	9.36	8.92	8.66
120	8.30	9.52	9.11	8.73
130	8.02	9.21	8.98	8.72
140	7.23	8.73	8.51	8.32
150	7.10	7.85	7.64	7.50
158	----	----	----	6.68
160	6.60	6.67	6.70	6.60
165	6.34	For fuselage stations 165 to 210.5 the body radii were the same as the unmodified fuselage.		
189.6	5.10			
195.6	4.50			
201.6	3.20			
204.6	2.30			
210.5	0			

Note: All dimensions are in inches. Nose-boom diameter, 1.50 inches.

NACA

TABLE II.- ZERO-LIFT DRAG-RISE COEFFICIENTS,  $\Delta C_{D_0}$ 

Modification	Computation or test	M=1.00	M=1.02	M=1.05	M=1.14
Unmodified	Theory, $C_{D_0}$ <sup>a</sup>	0.0244	0.0181	0.0164	0.0145
	Test, $\Delta C_{D_0}$	.0180	.0195	.0195	.0190
	Theory - Test	.0064	-.0014	-.0031	-.0045
	$\frac{\text{Theory} - \text{Test}}{\text{Test}} \times 100$ , percent <sup>a</sup>	35.5	-7.4	-15.9	-23.7
Modification 1 (for M=1.00)	Theory, $C_{D_0}$ <sup>a</sup>	.0115	.0135	.0162	.0224
	Test, $\Delta C_{D_0}$	.0094	.0144	.0158	<sup>b</sup> .0204
	Theory - Test	.0021	-.0009	.0004	.0020
	$\frac{\text{Theory} - \text{Test}}{\text{Test}} \times 100$ , percent	22.3	-6.3	2.5	9.8
Modification 2 (for M=1.05)	Theory, $C_{D_0}$ <sup>a</sup>	.0137	.0115	.0115	.0137
	Test, $\Delta C_{D_0}$	.0048	.0119	.0136	.0174
	Theory - Test	.0089	-.0004	-.0021	-.0037
	$\frac{\text{Theory} - \text{Test}}{\text{Test}} \times 100$ , percent	185.4	-3.4	-15.4	-21.3
Modification 3 (for M=1.14)	Theory, $C_{D_0}$ <sup>a</sup>	.0184	.0139	.0127	.0123
	Test, $\Delta C_{D_0}$	.0116	.0131	.0139	.0151
	Theory - Test	.0068	.0008	.0012	.0028
	$\frac{\text{Theory} - \text{Test}}{\text{Test}} \times 100$ , percent	56.7	6.1	-8.6	-18.5
Instrument accuracy for tests of modifications		$\pm 0.0004$	----	----	$\pm 0.0002$

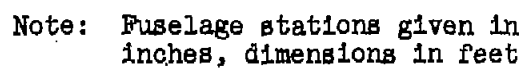
<sup>a</sup>Indication of disagreement between theory and experimentation.<sup>b</sup>Estimated from extension of experimental data from M=1.126.

NACA

TABLE III.- IMPROVEMENT IN ZERO-LIFT DRAG-RISE COEFFICIENT  
EFFECTED BY THE SEVERAL MODIFICATIONS

Modification Compared	Computation or Test	M=1.00	M=1.02	M=1.05	M=1.14
Unmodified - Modification 1 (for M=1.00)	Theory, $\Delta(C_{D_0}')$	0.0129	0.0046	0.0002	-0.0079
	Test, $\Delta(\Delta C_{D_0})$	.0086	.0051	.0037	-.0014
	Theory - Test	.0043	-.0005	-.0035	-.0065
Unmodified - Modification 2 (for M=1.05)	Theory, $\Delta(C_{D_0}')$	.0107	.0066	.0049	.0008
	Test, $\Delta(\Delta C_{D_0})$	.0132	.0076	.0059	.0016
	Theory - Test	-.0025	-.0010	-.0010	-.0008
Unmodified - Modification 3 (for M=1.14)	Theory, $\Delta(C_{D_0}')$	.0060	.0042	.0037	.0023
	Test, $\Delta(\Delta C_{D_0})$	.0064	.0064	.0056	.0039
	Theory - Test	-.0004	-.0022	-.0019	-.0016
Modification 2 - Modification 3	Theory, $\Delta(C_{D_0}')$	-.0047	-.0024	-.0012	.0015
	Test, $\Delta(\Delta C_{D_0})$	-.0068	-.0012	-.0003	.0023
	Theory - Test	.0021	-.0012	-.0009	-.0008
Instrument accuracy for tests of modifications		$\pm .0004$	----	----	$\pm .0002$

NACA



$$\frac{r}{r_0} = \left[ 1 - \left( \frac{x-102}{102} \right)^2 \right]^{3/4}$$

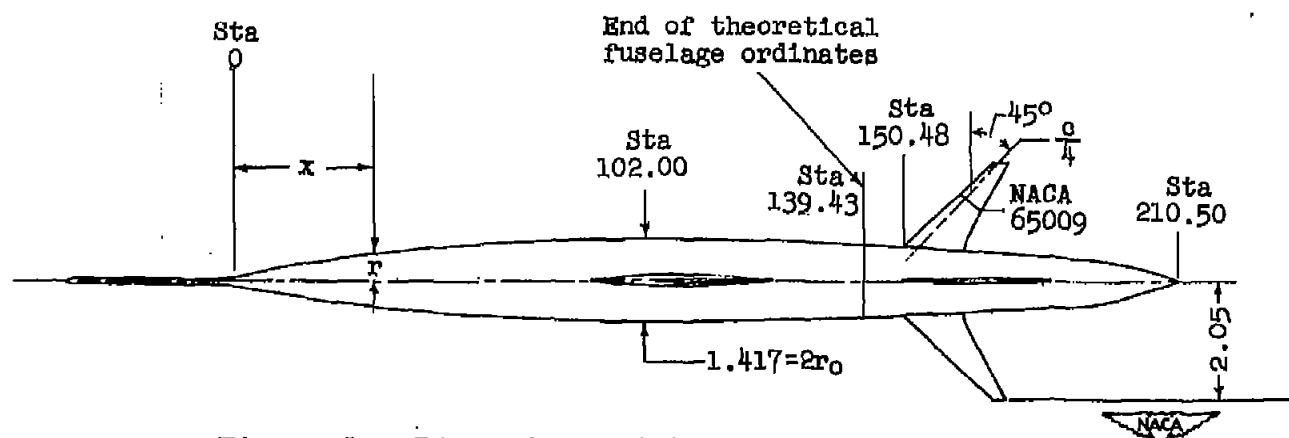


Figure 1.- Dimensions of the unmodified model.

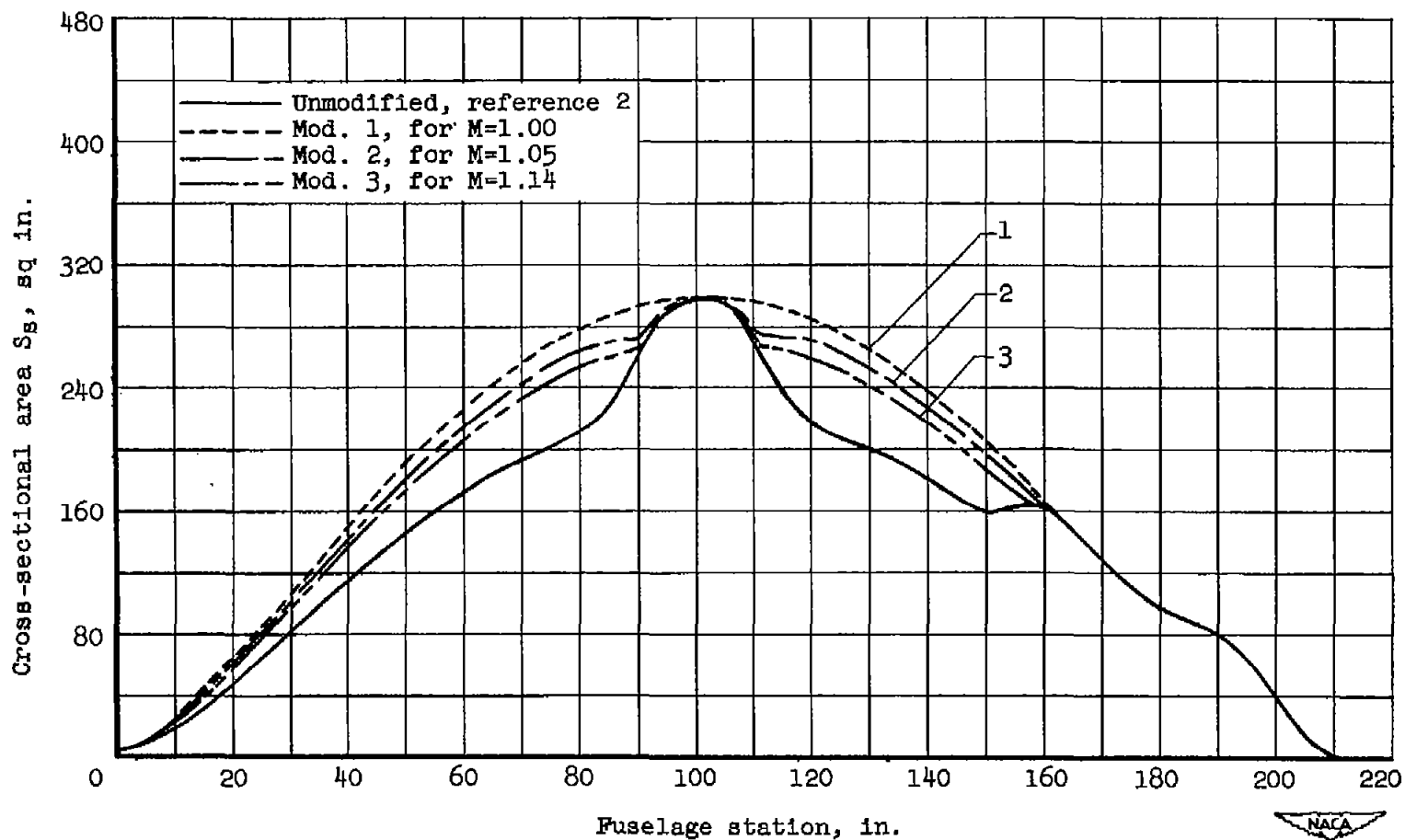
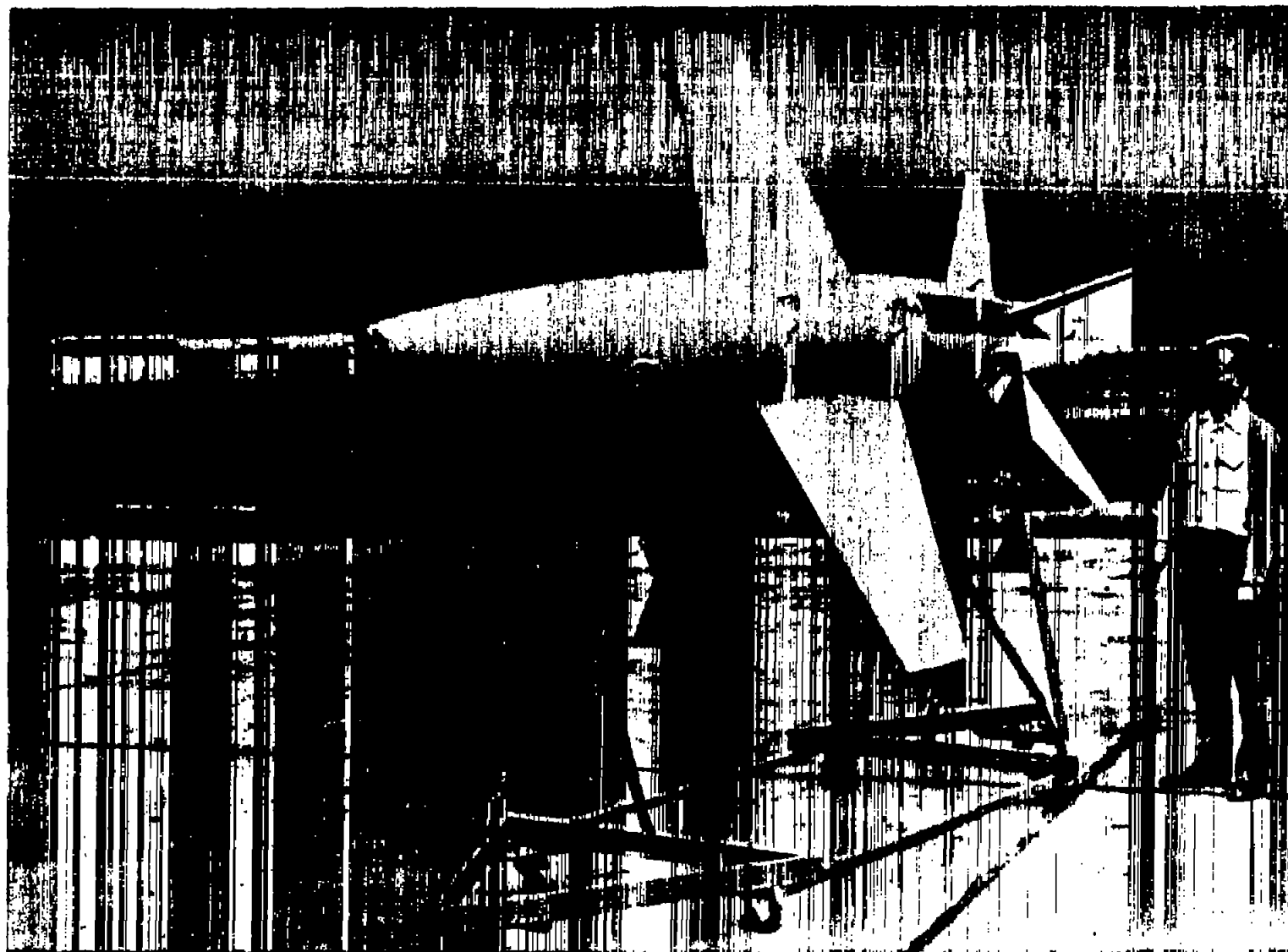


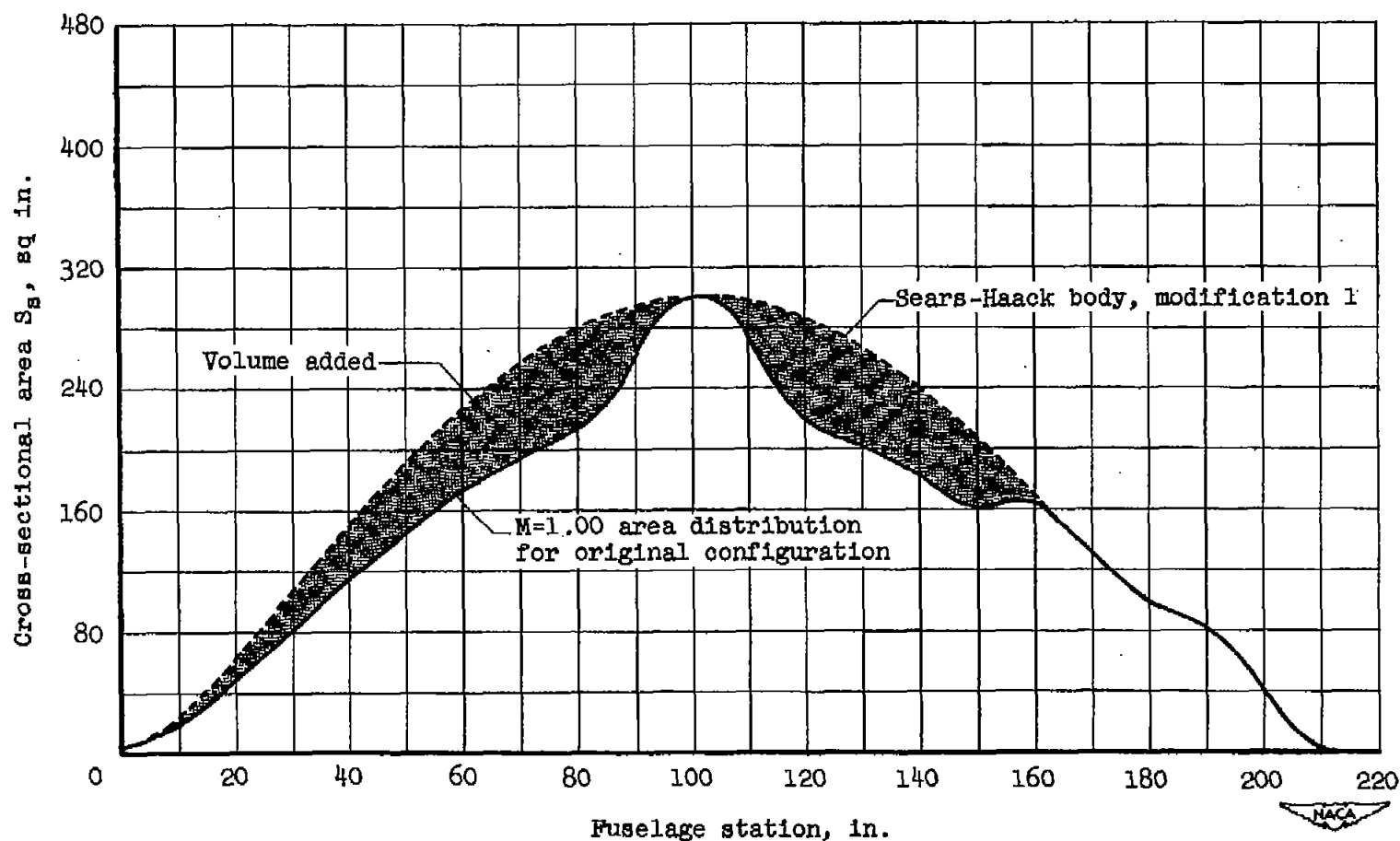
Figure 2.- The axial distributions of cross-sectional area normal to the longitudinal axis for the basic model and for the three modifications.



A-16822

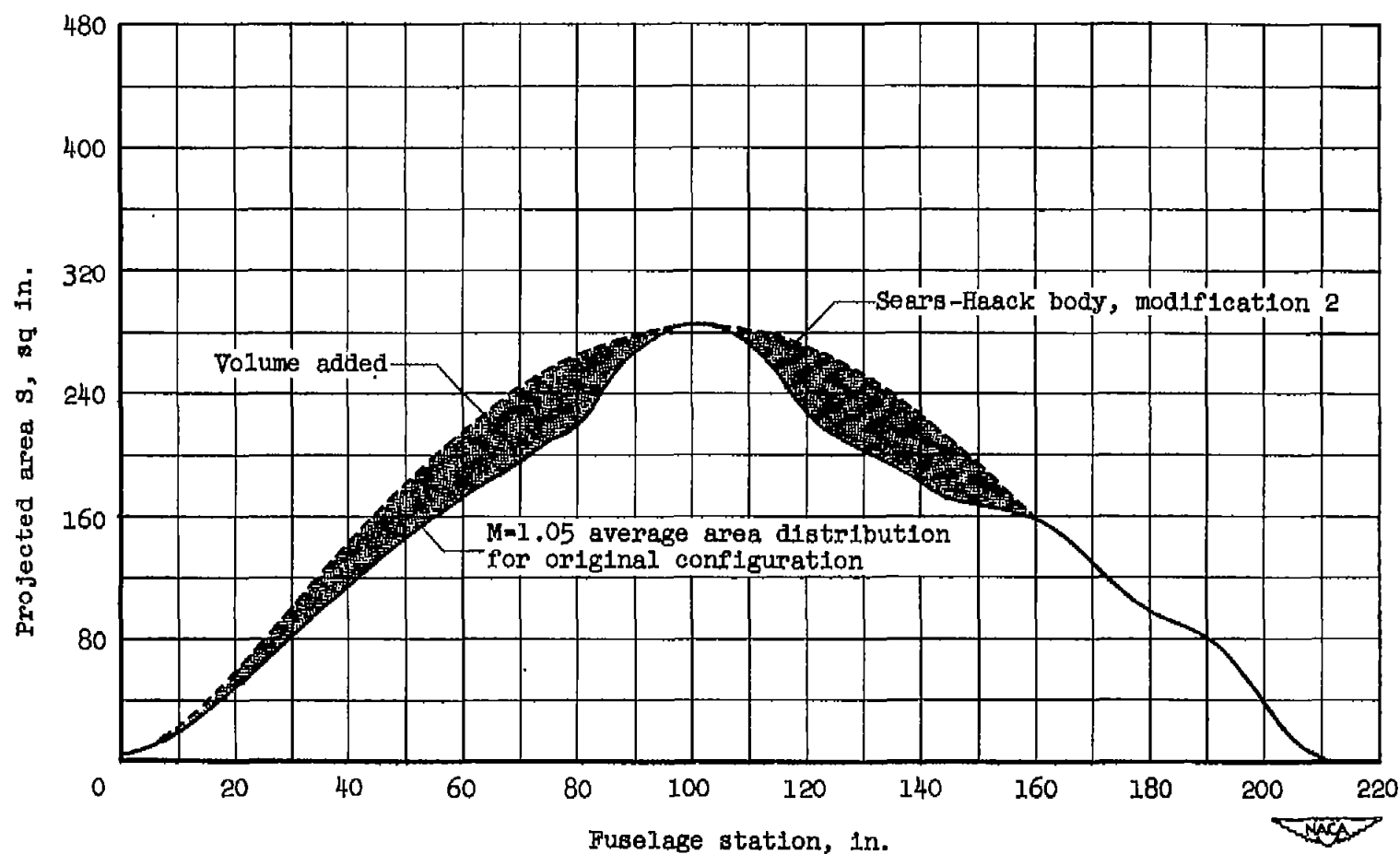
Figure 3.- Model modified for  $M=1.00$ . The airplane attachment brackets were retracted to form a flush surface during free-fall flight.





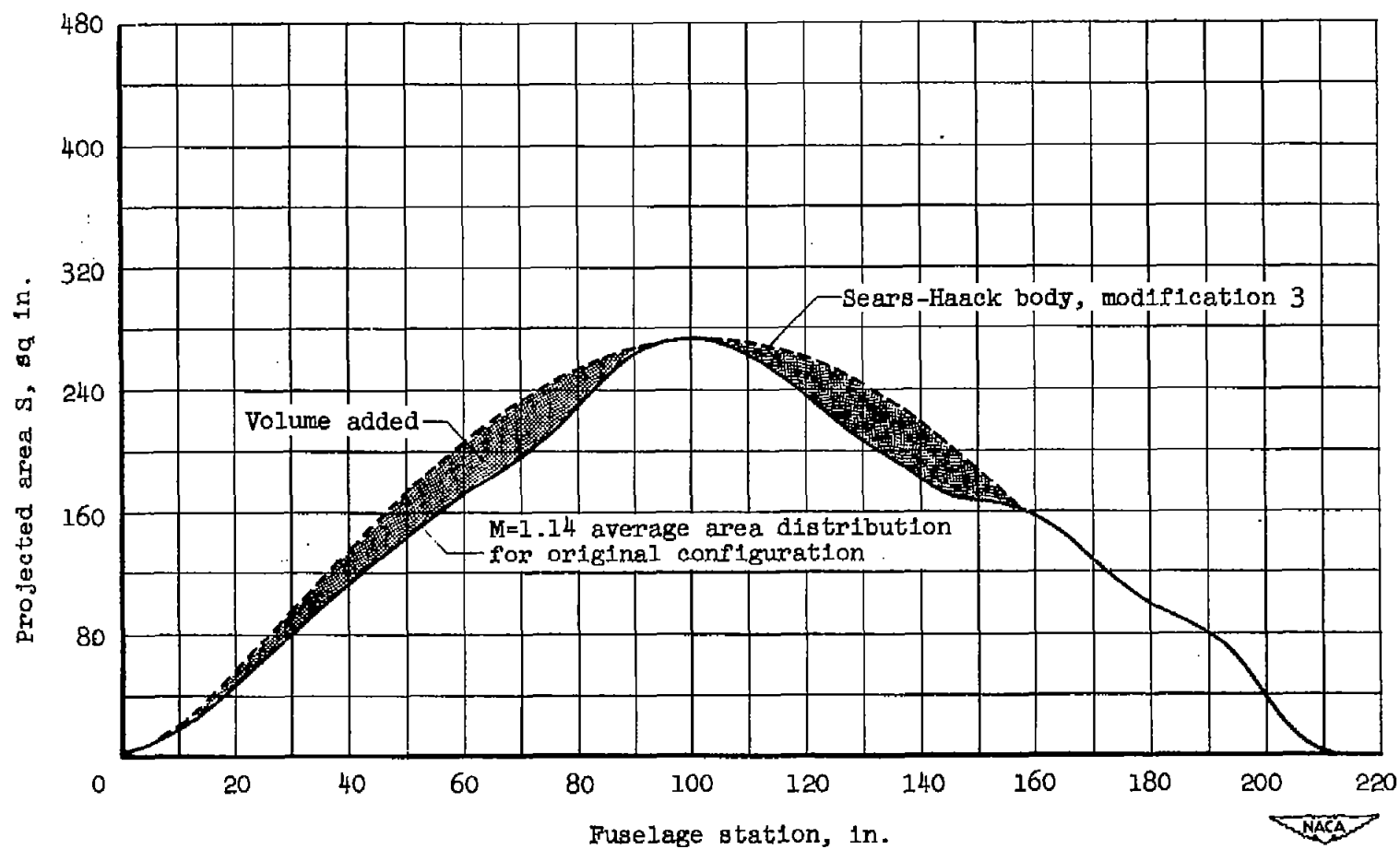
(a) Modification 1, for  $M=1.00$ .

Figure 4.- Volume added to the fuselage for the various modifications.



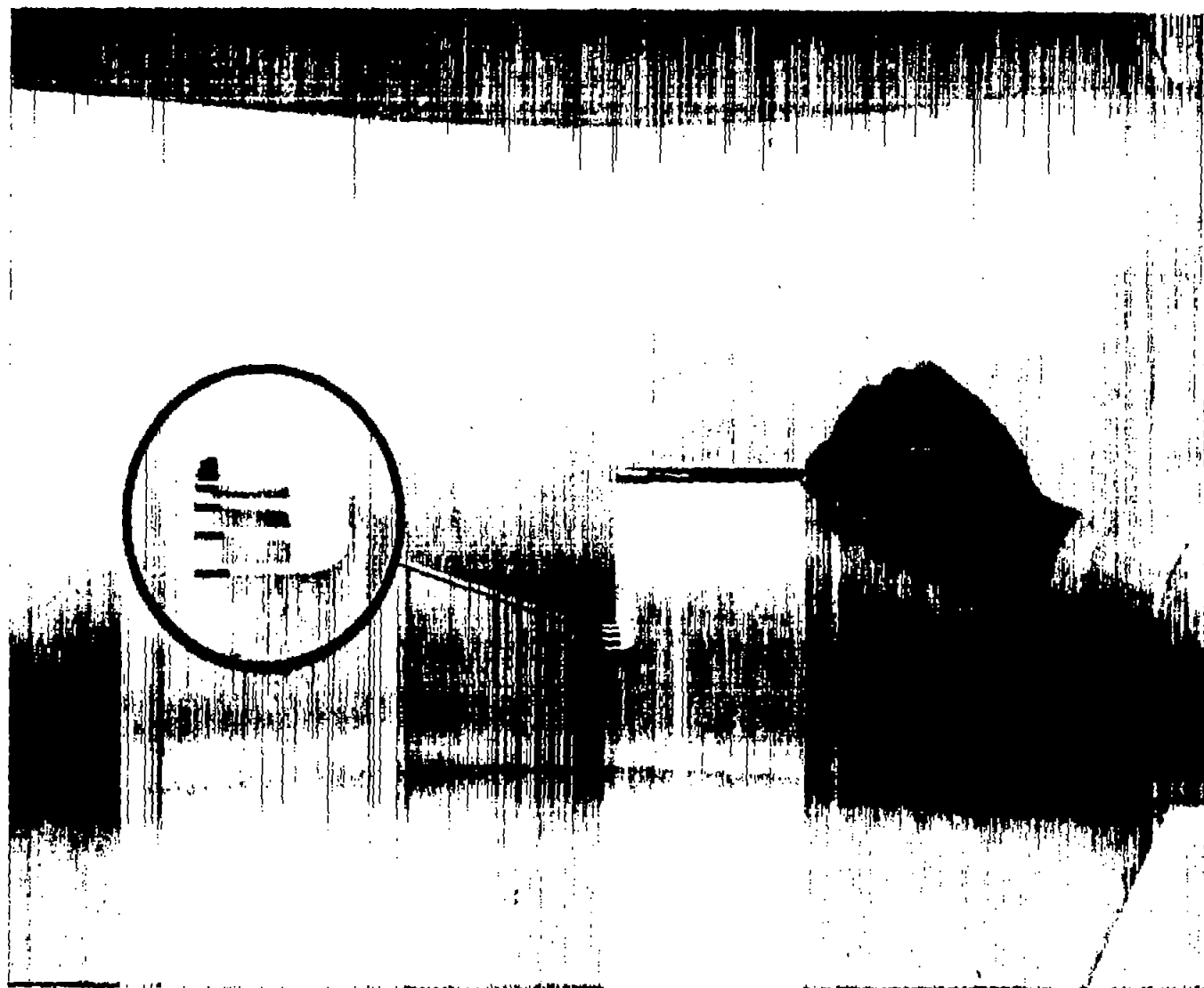
(b) Modification 2, for  $M=1.05$ .

Figure 4.- Continued.



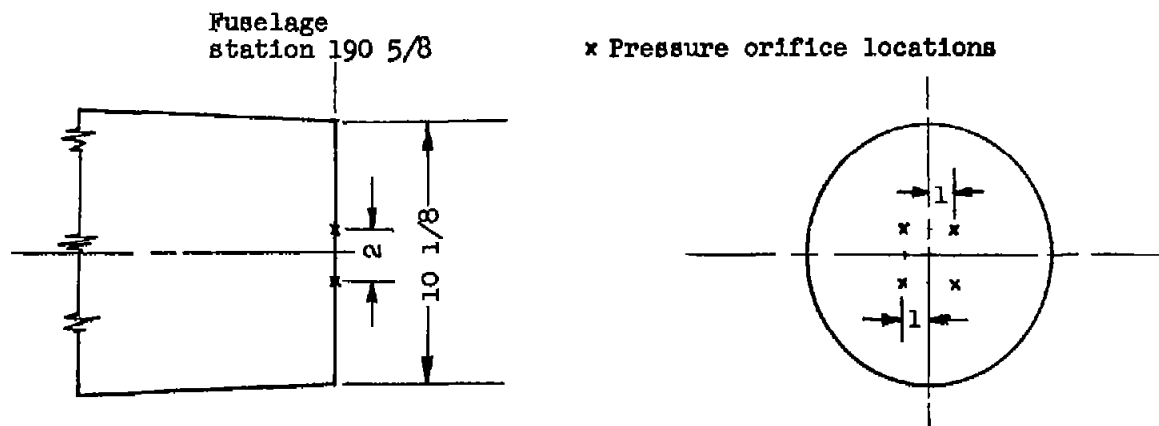
(c) Modification 3, for  $M=1.14$ .

Figure 4.- Concluded.

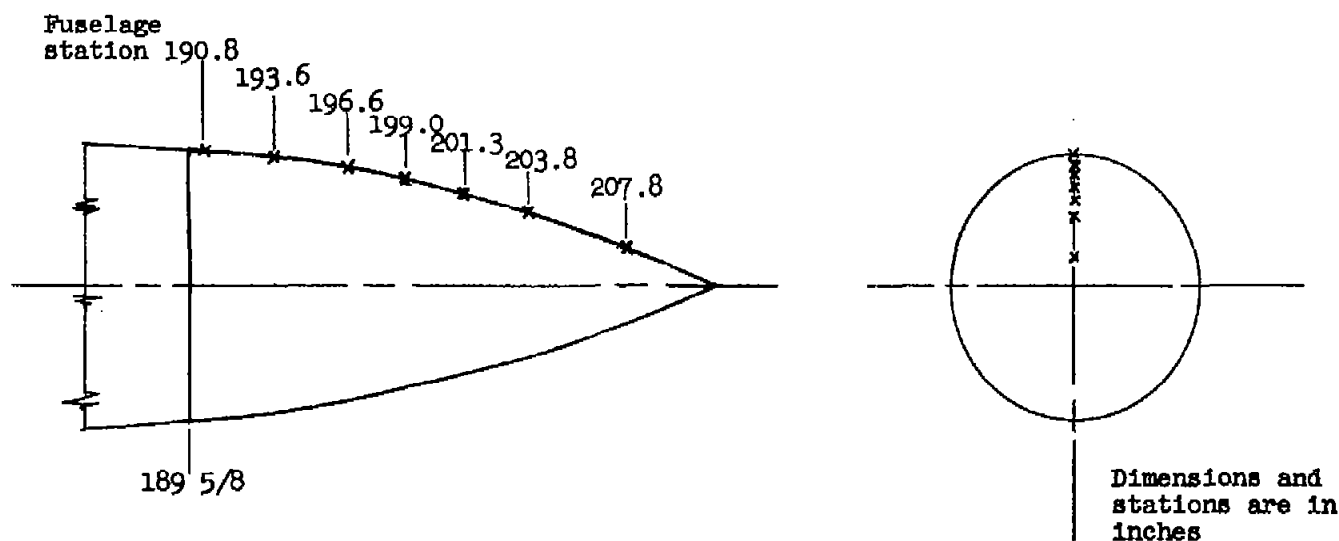


A-18829.1

Figure 5.- Four-tube pitot-pressure rake located at fuselage station 100.



(a)  $M=1.05$  modification with blunted tail.



(b) Modification 3, for  $M=1.14$ .

Figure 6.- Tail configuration and pressure orifice locations for the two drop tests in which base pressures were determined.

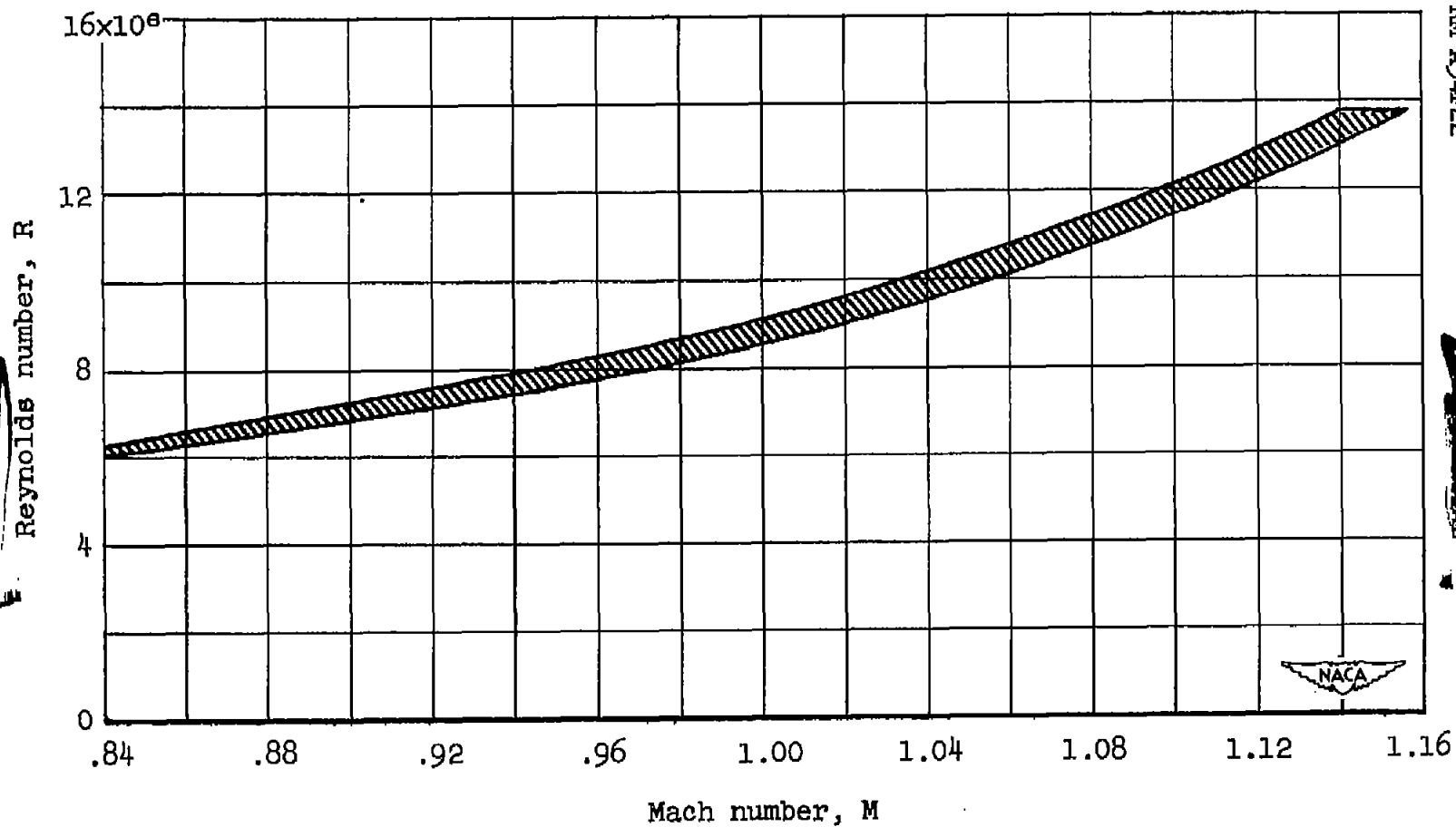
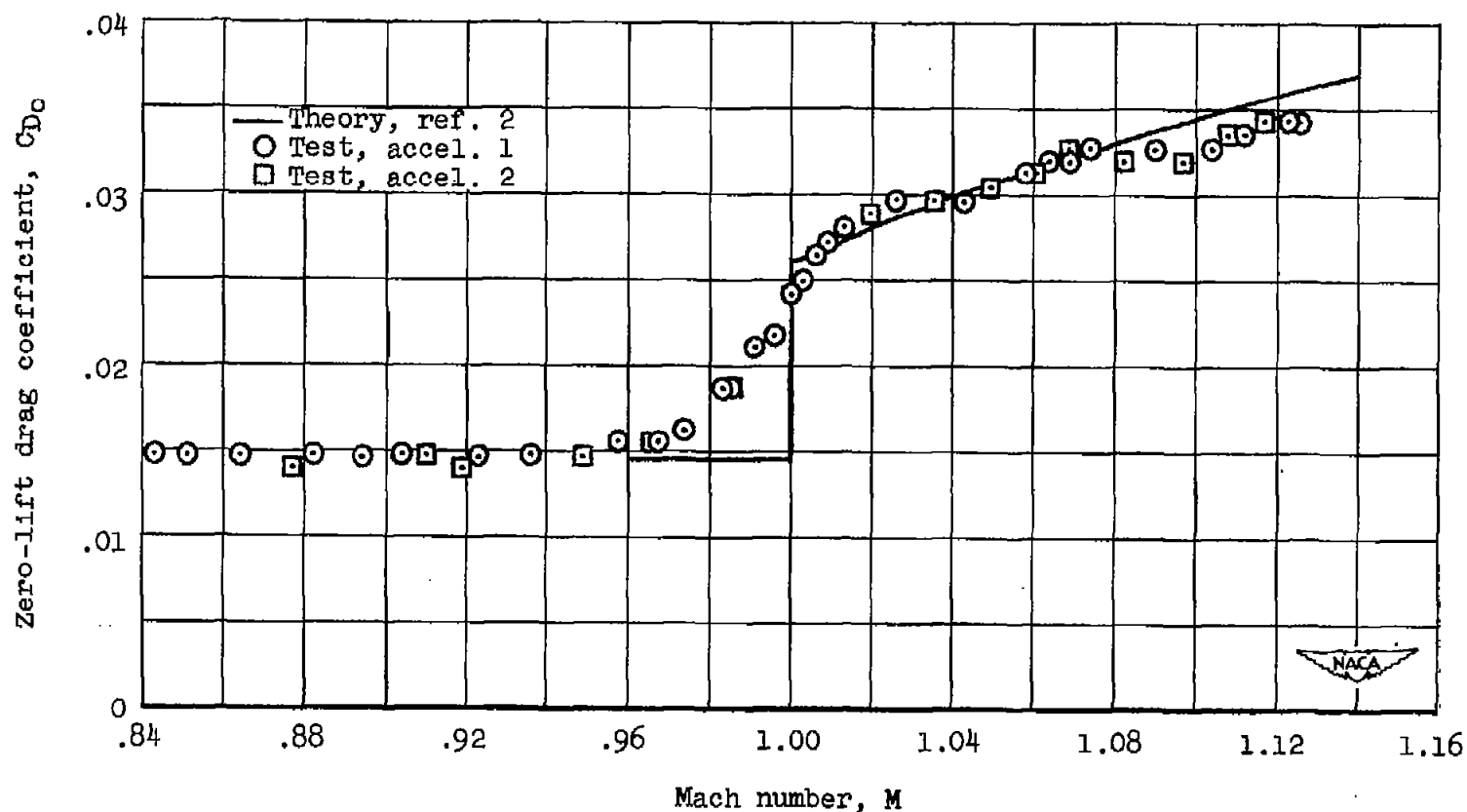


Figure 7.- Reynolds number variation with Mach number for the tests of the modified configurations.



(a) Modification 1, for  $M=1.00$ .

Figure 8.- Comparison of experimental zero-lift drag coefficients with the theoretical wave-drag coefficients from reference 2 added to the subsonic level of the experimental data.

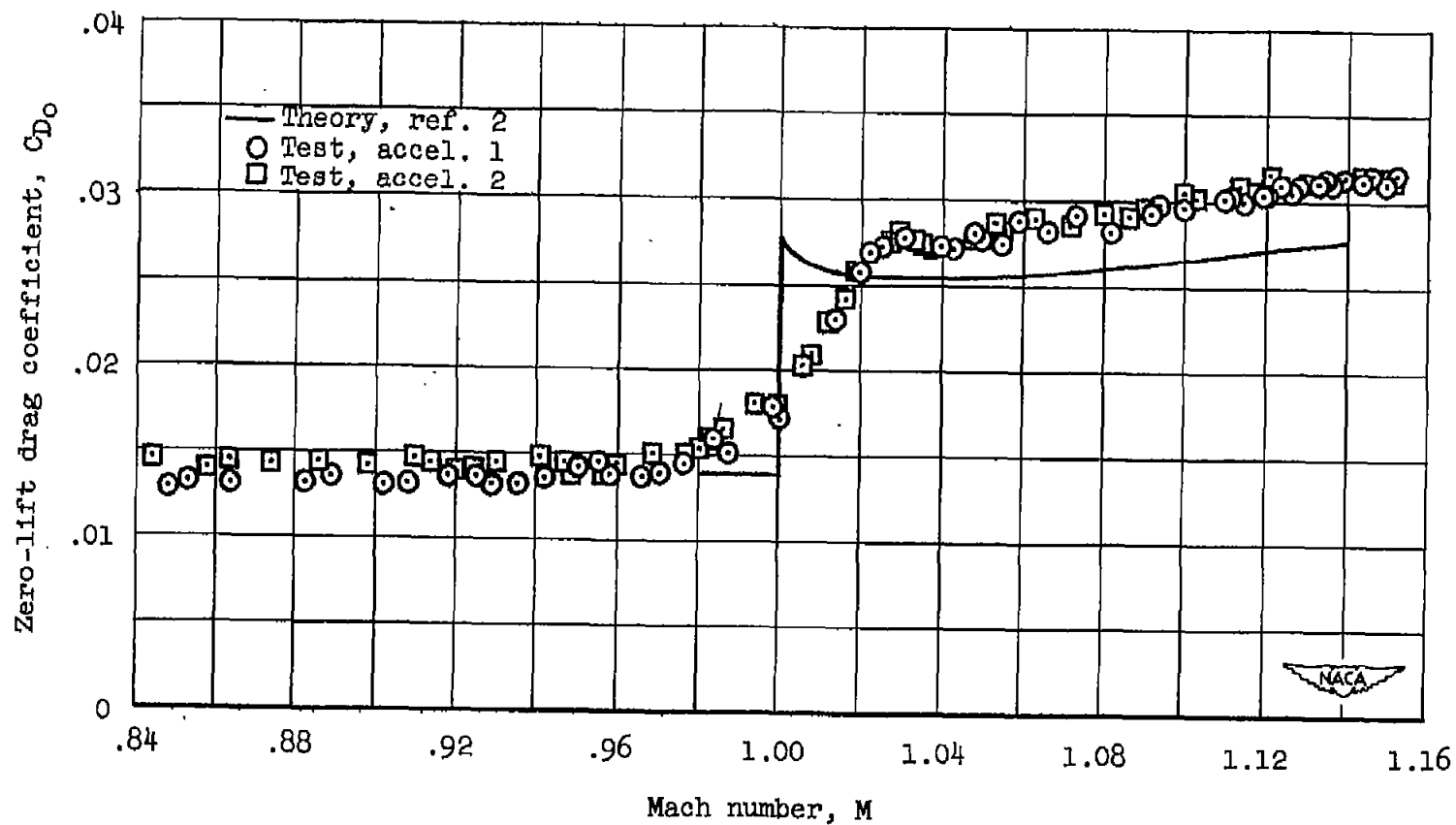
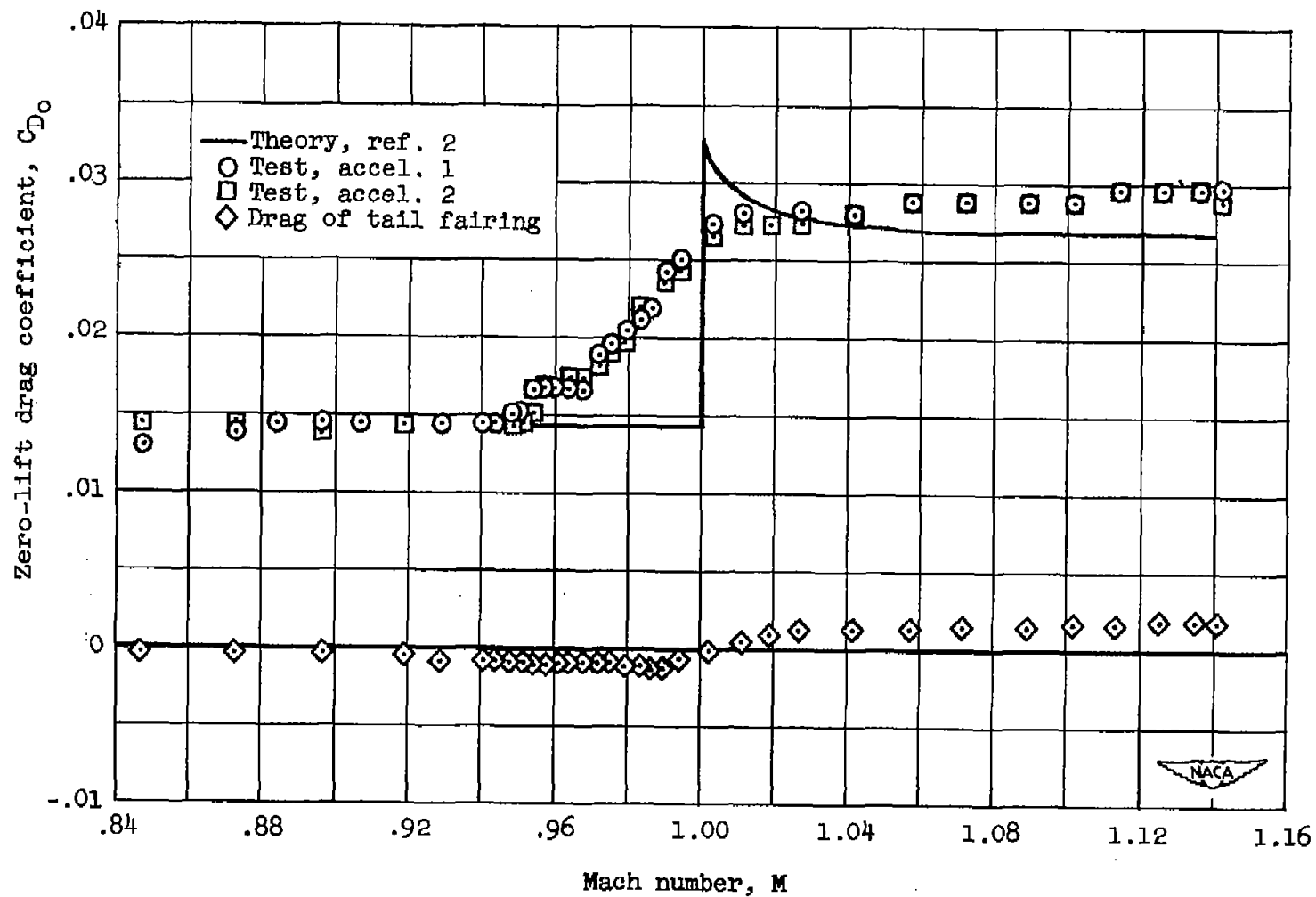
(b) Modification 2, for  $M=1.05$ .

Figure 8.- Continued.





(c) Modification 3, for  $M=1.14$ .

Figure 8.- Concluded.

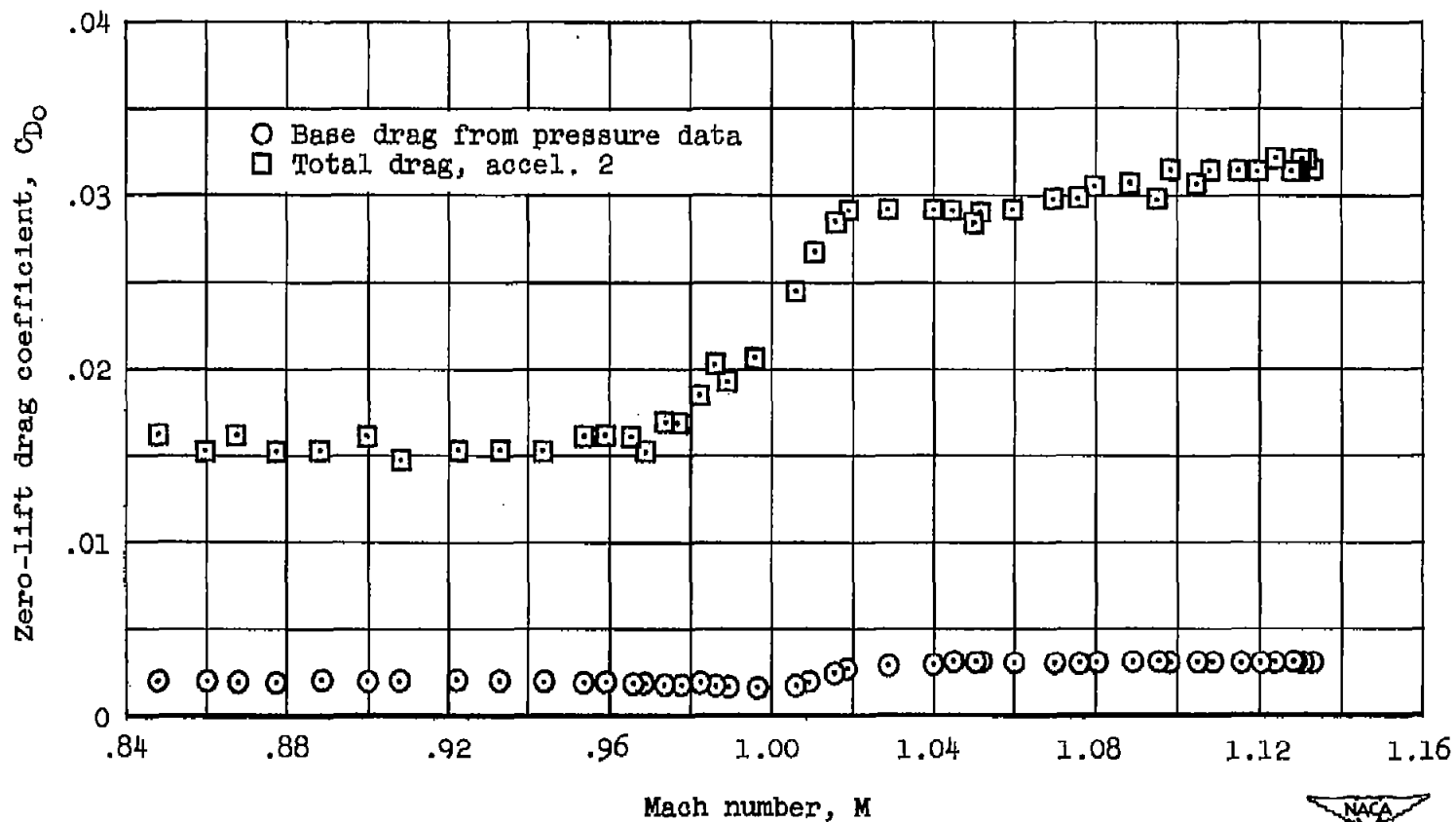


Figure 9.- Experimental zero-lift drag coefficients for modification 2, for  $M=1.05$ , with tail fairing behind station 190-5/8 cut off to form a flat base.

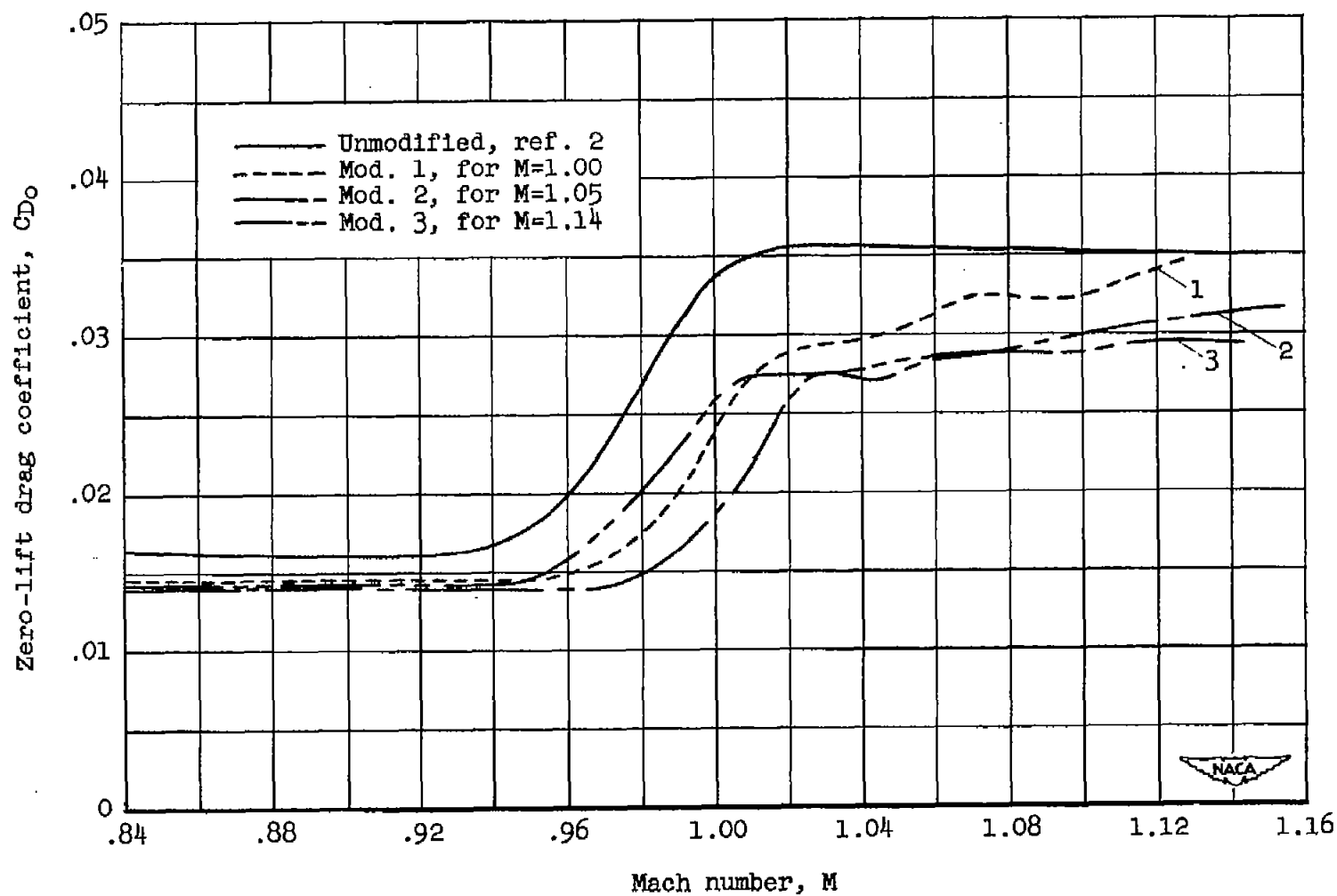


Figure 10.- Comparison of the experimental zero-lift drag coefficients for the various modifications with the unmodified configuration.

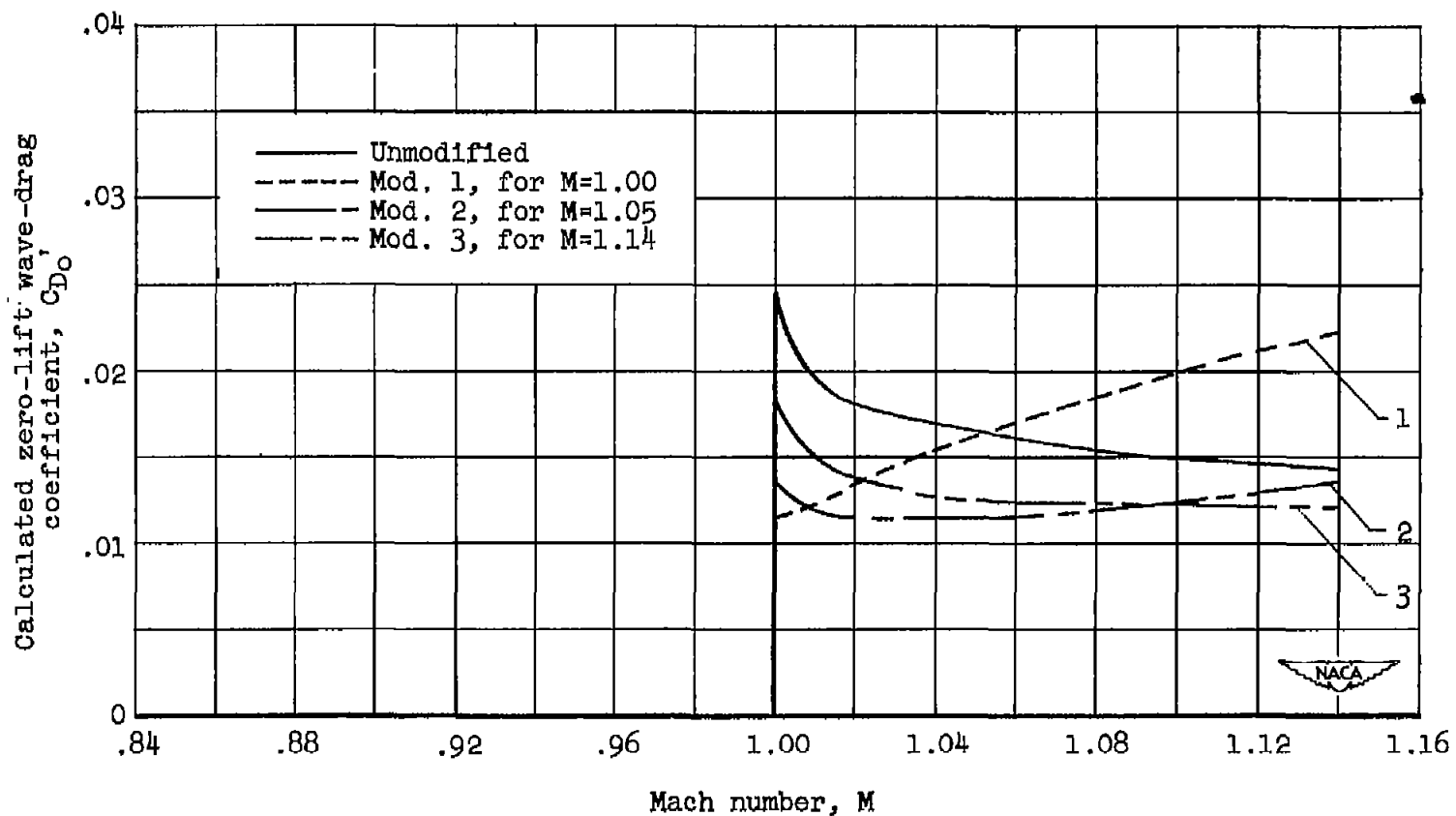
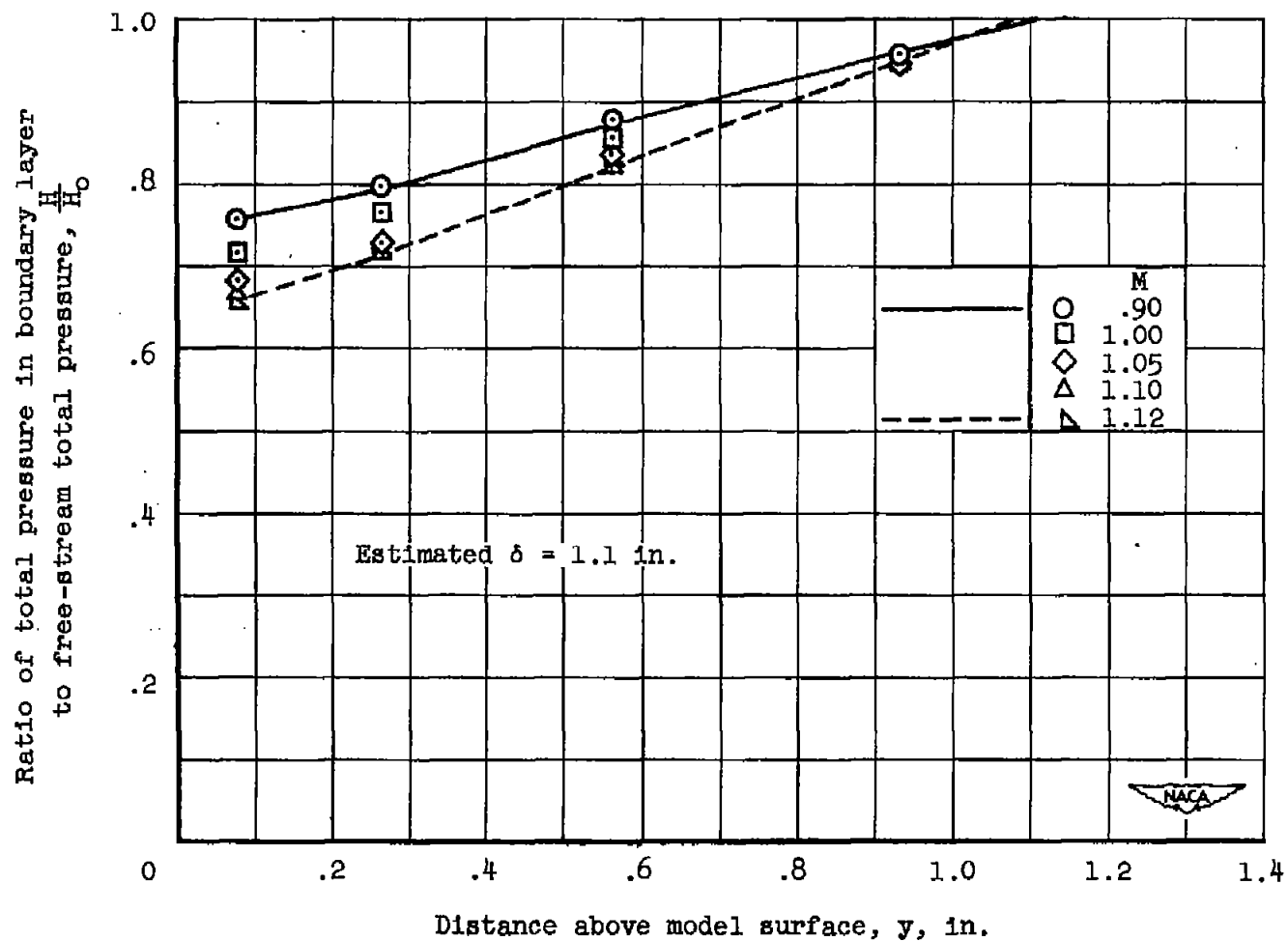
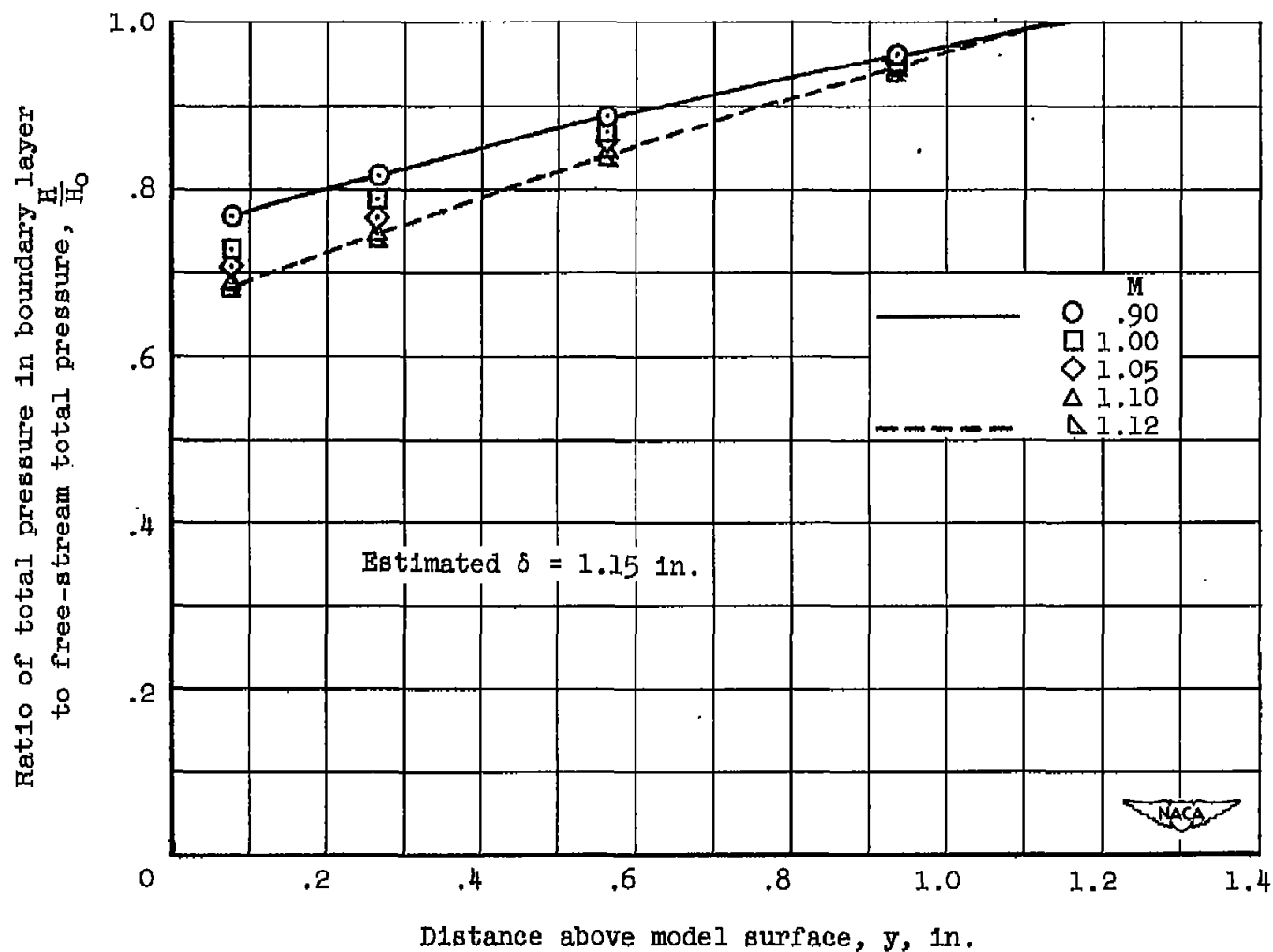


Figure 11.- Theoretical computations from reference 2.



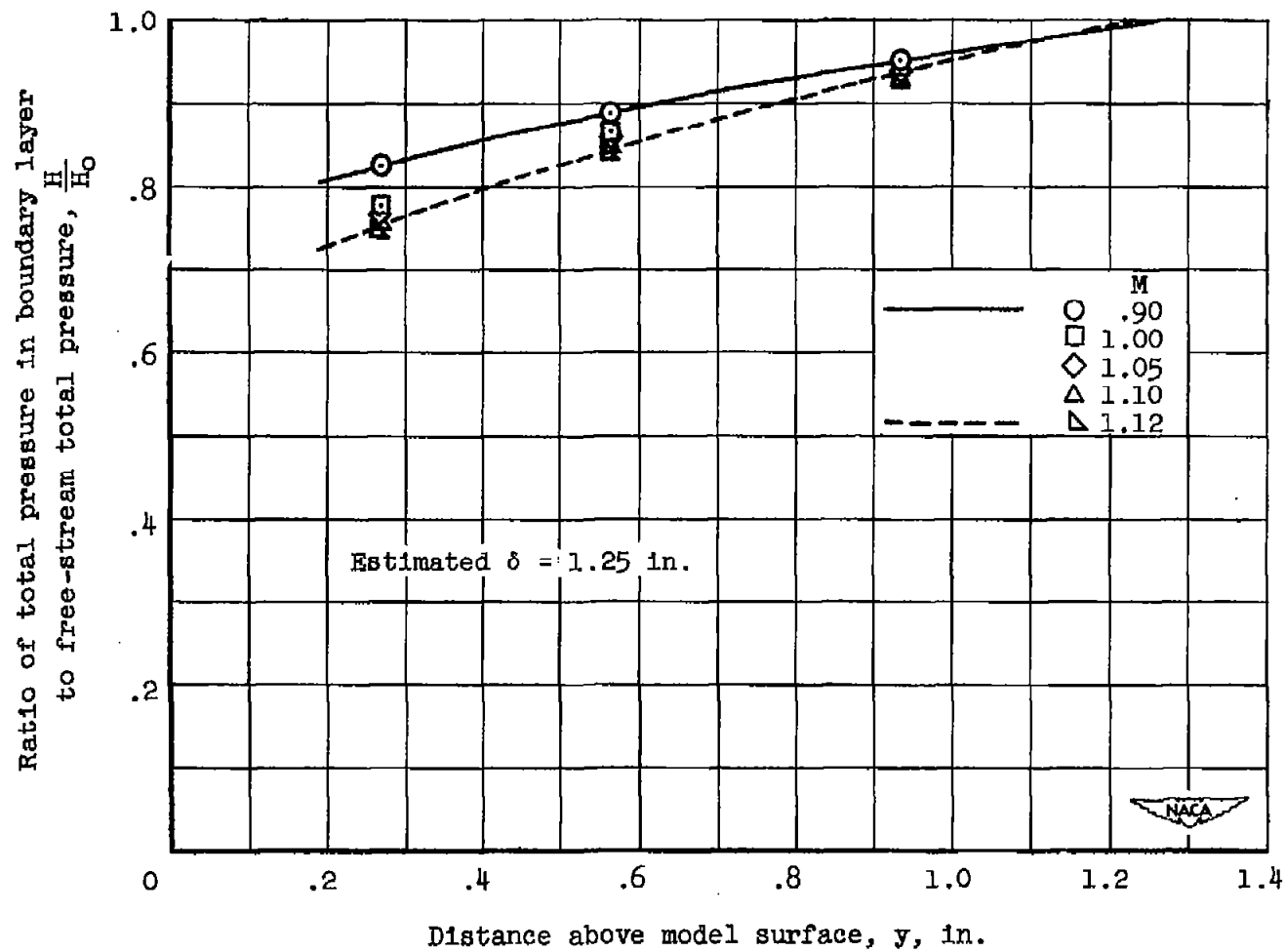
(a) Modification 1, for  $M=1.00$ .

Figure 12.- Total pressure distribution in the boundary layer measured at fuselage station 100.



(b) Modification 2, for  $M=1.05$ .

Figure 12.- Continued.



(c) Modification 3, for  $M=1.14$ .

Figure 12.- Concluded.

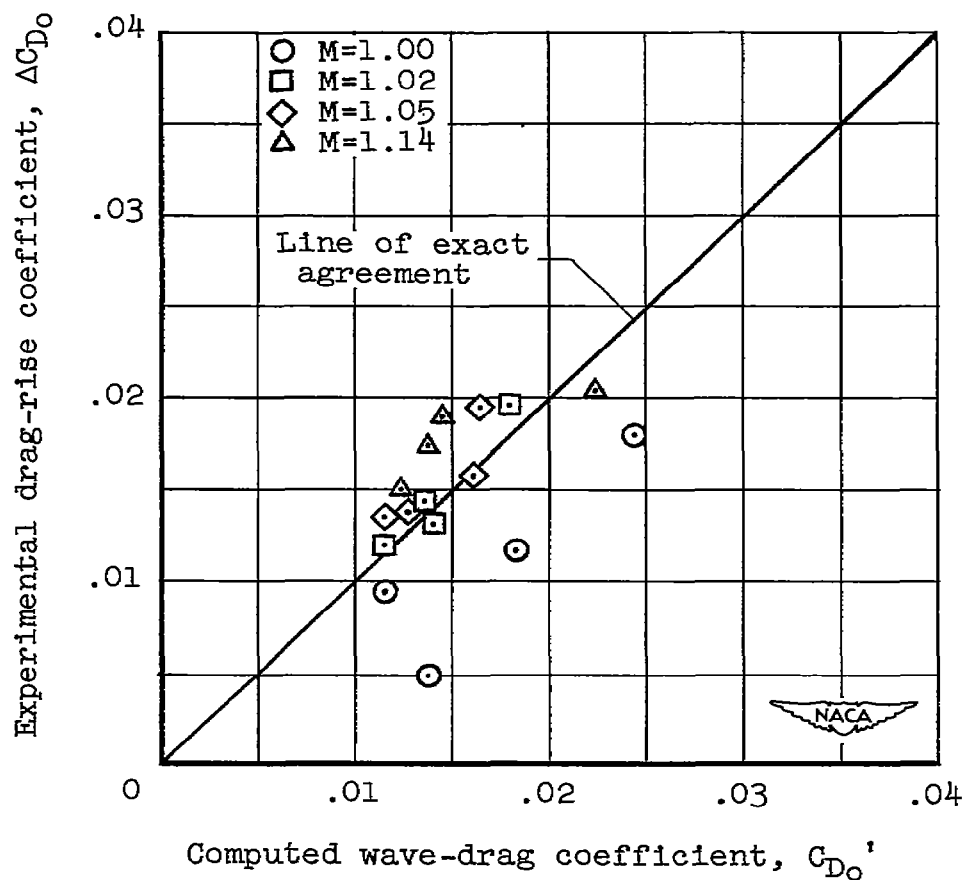


Figure 13.- Comparison between computed zero-lift wave-drag coefficients and experimental zero-lift drag-rise coefficients (see table II).



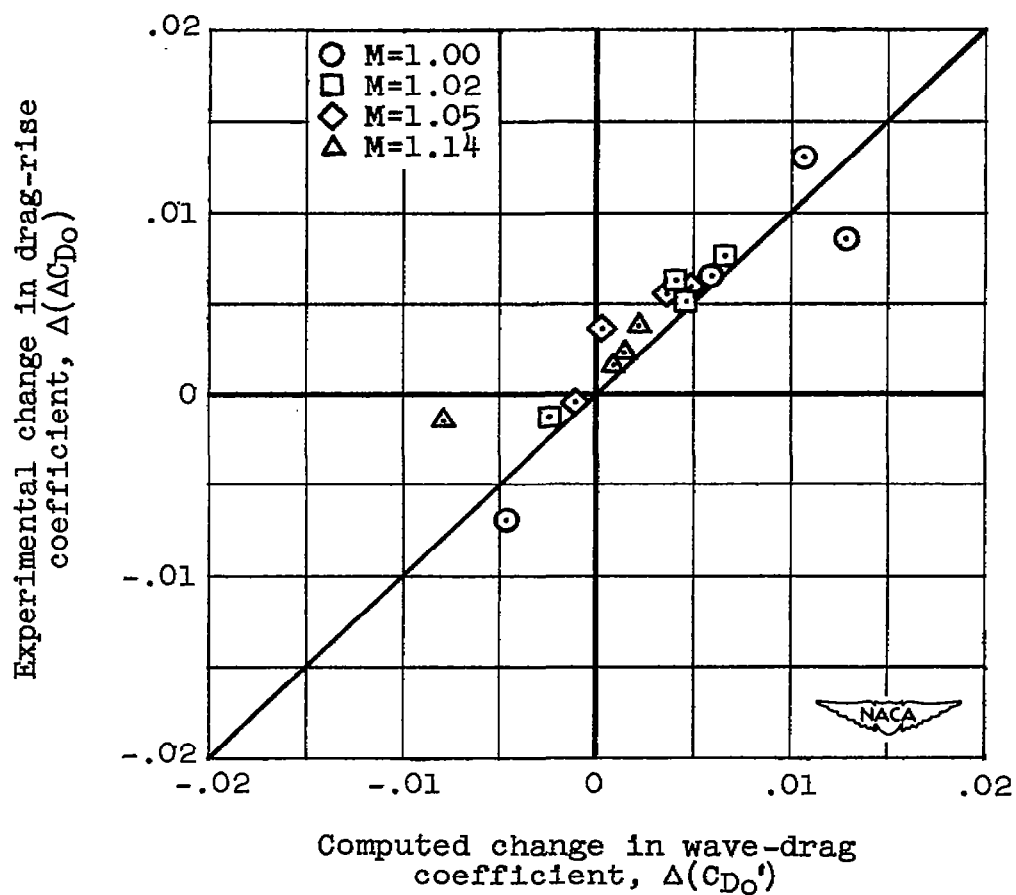
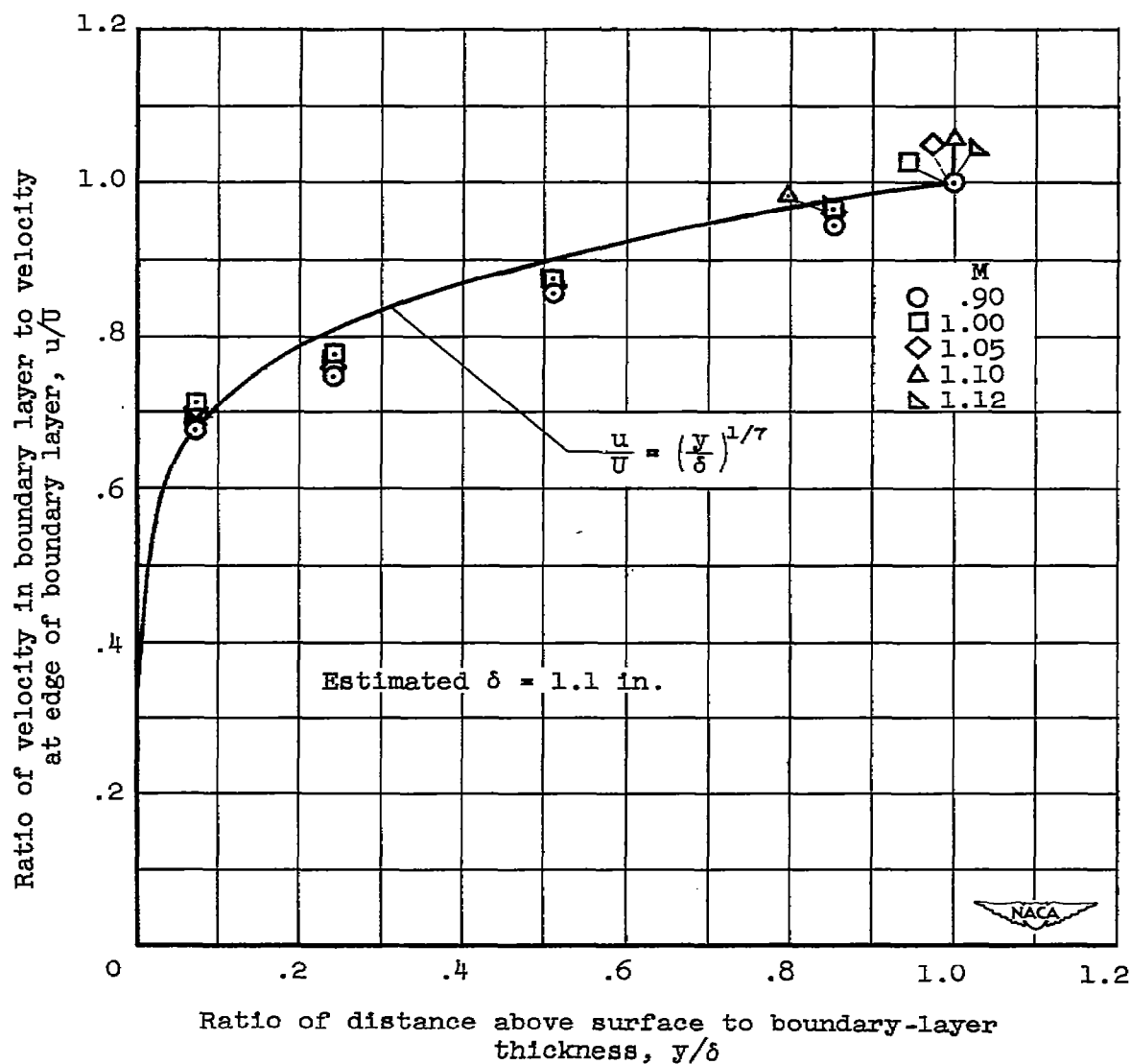
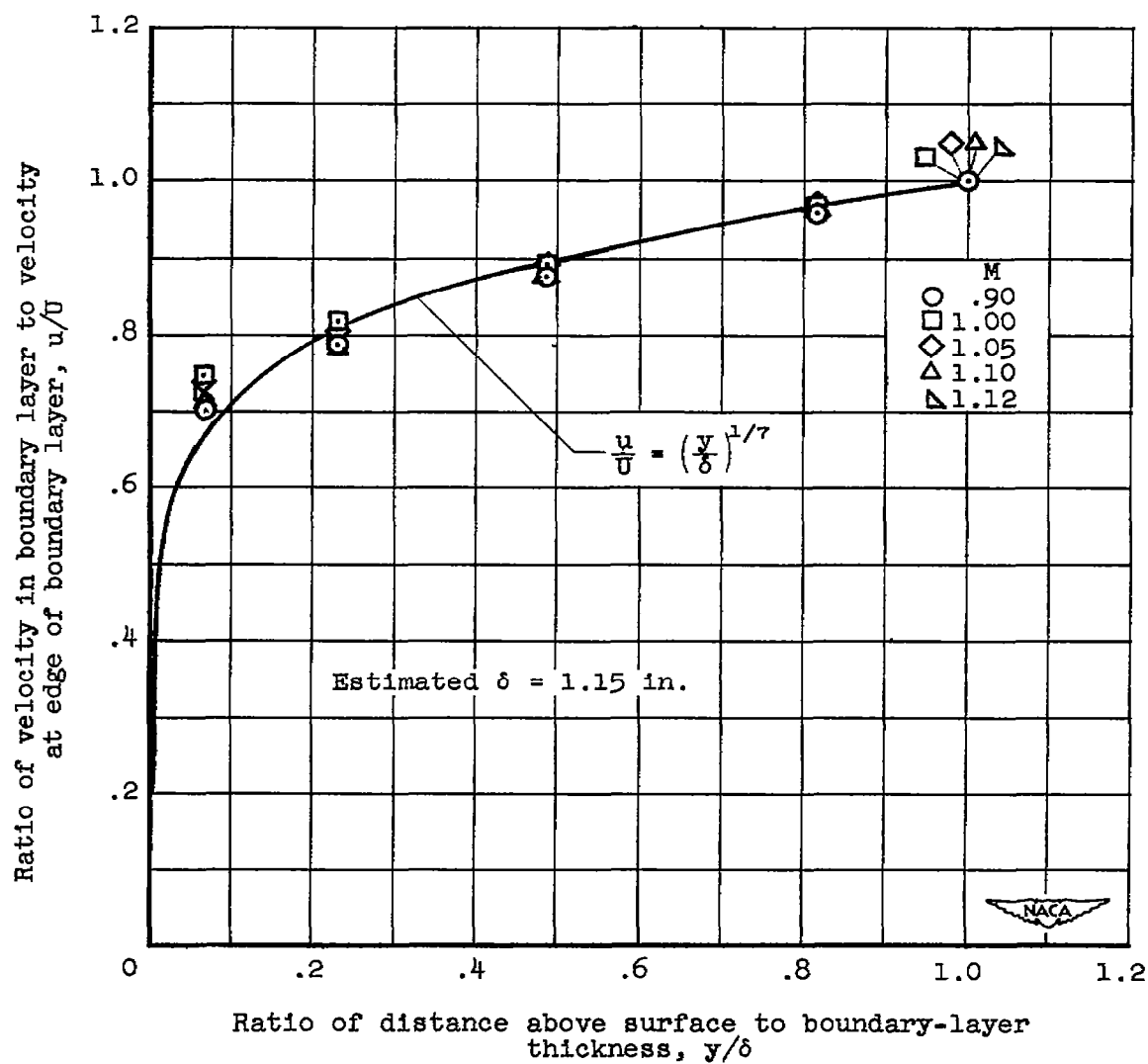


Figure 14.- Comparison between changes in computed zero-lift wave-drag coefficients and changes in experimental zero-lift drag-rise coefficients due to modifications (see table III).



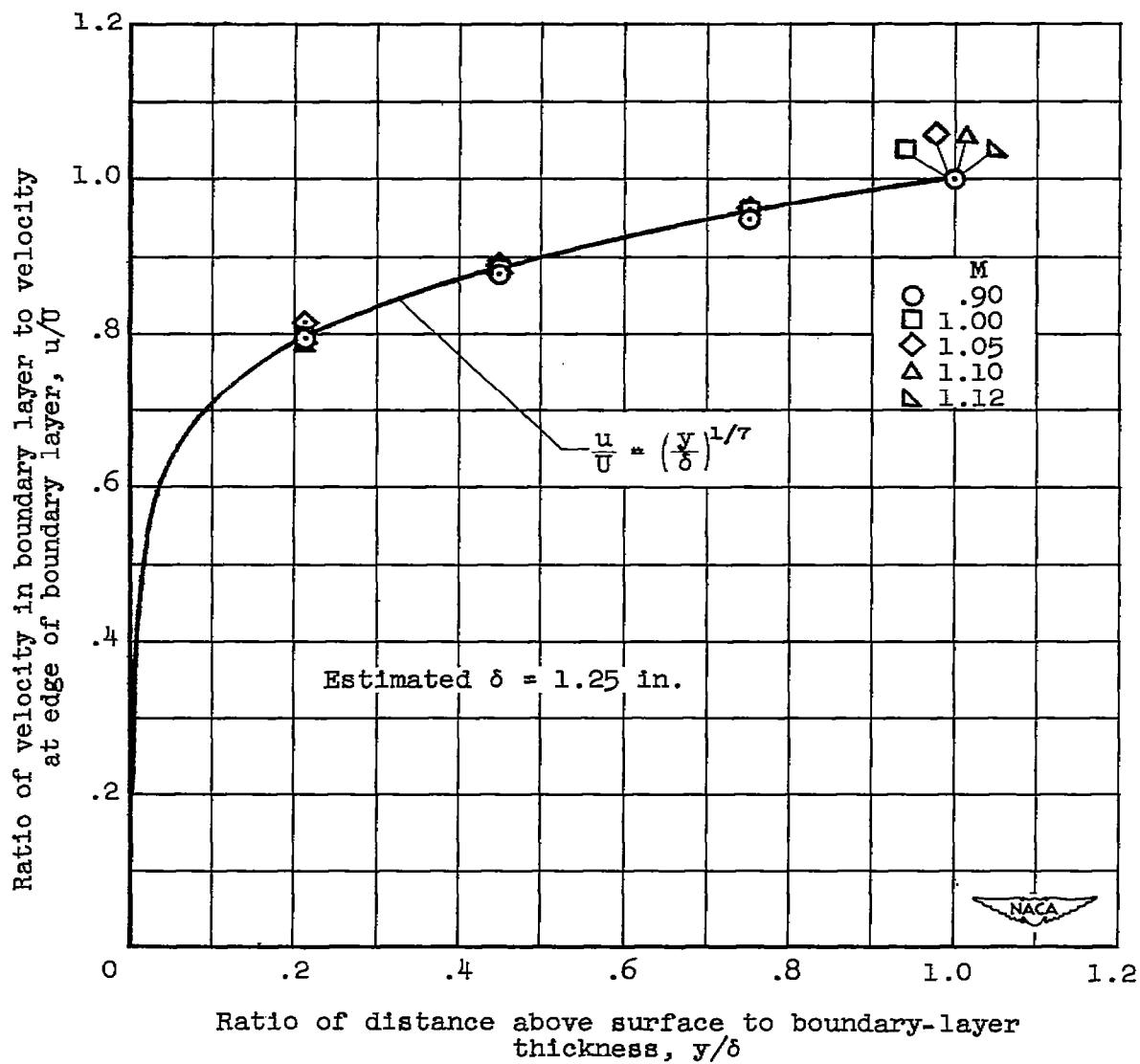
(a) Modification 1, for  $M=1.00$ .

Figure 15.- Velocity profile data points in the turbulent boundary layer at fuselage station 100.



(b) Modification 2, for  $M=1.05$ .

Figure 15.- Continued.



(c) Modification 3, for  $M=1.14$ .

Figure 15.- Concluded.

~~CONFIDENTIAL~~

LANGLEY RESEARCH CENTER



3 1176 01355 2121

~~CONFIDENTIAL~~